



High-Pressure Thermodynamic Properties of Fatty Acids Methyl Esters as Renewable Fuel

Rachid AITBELALE^{1,2*}, Ilham ABALA^{1,2}, Mohamed LIFT^{2,3}, Younes CHHITI⁴,
Fatima Ezzahrae M'HAMDI ALAOUI², Abdelaziz SAHIBED-DINE¹

¹Laboratory of Catalysis and Corrosion of Materials (LCCM), Chemistry Department, Chouaïb Doukkali University, El Jadida, Morocco

²Science Engineer Laboratory for Energy (LabSIPE), National School of Applied Sciences, Chouaïb Doukkali University, El Jadida, Morocco

³Department of Electromechanical Engineering, Escuela Politécnica Superior, Burgos University, E-09006 Burgos, Spain

⁴National School of Chemistry, Ibn Tofaïl University, Kenitra, Morocco

*Corresponding author Email: aitbelale.rachid@yahoo.fr

Abstract Biodiesel is a mixture of monoalkyl esters of long chain fatty acids. The knowledge of the thermodynamic properties of fatty acids methyl esters (FAME) leads to know some biodiesel thermo-physical properties. The main aim of this work is to analyze the density correlation of seven FAME listed as follows: Methyl laurate (12:0), Methyl myristate (14:0), Methyl palmitate (16:0), Methyl stearate (18:0), methyl oleate (18:1), methyl linoleate (18:2) and methyl linolenate (18:3) between 270K and 393.15K and for pressures up to 80 MPa. For that, the PR, Tait and PC-SAFT equations of state (EoS) have been used. When using the PR equation of state, the critical parameters: T_c , p_c and acentric factor ω were selected using a comparative study based on several previous works of literature. However, the Tait equation was fitted to the experimental density data for each compound (FAME) and for the PC-SAFT equation, the characteristic parameters related to each ester have been estimated by adjusting the equation to the experimental data. In order to compare the experimental density values with those obtained with the correlation considered in this work, we have used the Absolute Average Deviation, AAD. The Tait equation and PC-SAFT equation showed effectiveness to correlate the density, whereas, the PR equation is not appropriate to correlate the density of complex long-chain fluids. Moreover, the derived thermodynamic properties, such as the isothermal compressibility, κ_T , and isobaric thermal expansivity, α_p , have been derived from the Tait equation. The same behavior is observed for, κ_T , and, α_p , as a function of pressure and temperature and the effect of alkyl chain length was revealed. The isotherms, α_p , of FAME showed a point of intersection as expected, which means that α_p was independent of the temperature in this pressure.

Keywords Biodiesels, PC-SAFT EoS, FAME, Thermodynamic properties, density

1. Introduction

Due to the environmental impacts and high prices of fossil diesel, biodiesel has been the subject of a great deal of attention in recent years because it is biodegradable, non-toxic and renewable [1]. Biodiesels are defined as a

mixture of fatty acids mono-alkyl esters of long-chain, products from vegetable and/or animal oils according to the American Society of Testing and Materials (ASTM D 6751) [2]. A large number of studies have shown that biodiesel is a potential alternative of fossil fuel [3]. Numerous studies have attempted to develop models to quantify the relationship between the operating conditions and the performance of the process. To simulate the mass and energy balances, it is essential to know four fundamental thermophysical properties: the liquid density (ρ_{liq}), the saturation pressure (P_{sat}), the liquid heat capacity ($C_{p(liq)}$) and the vaporization enthalpy (H_{vap}) [4]. This work presents the correlation of density results of same FAME using the Tait, PR and PC-SAFT EoS, based on the literature experimental data [5-9].

In order that biodiesel can replace the diesel, it must be produced on a large scale. For this purpose, it requires specific information on thermodynamic properties. It is very difficult to measure these properties for biodiesel because they are formed by high molecular weight components and complex structures. Therefore, it is necessary to develop models that predict these properties [10], for example, the prediction of the phase equilibria of the ternary biodiesel + glycerol + alcohol reactive system is essential to design and optimize the conditions of trans-esterification reactors [11-13]. In order to predict accurately the phase equilibrium, it is necessary to use thermodynamic models.

Ferreira *et al.* [14] studied the contribution of groups associated with the equation of state to represent the phase equilibria of mixtures containing acids, esters and ketones with water, alcohol and inert compounds. The authors have found a good representation of pure component properties and phase equilibria for mixtures of carboxylic acids with inert compounds, alcohols, and water at both low and high pressures.

Pena *et al.* [15] performed bibliographic research of phase equilibrium data of high pressure carbon dioxide reagents and enzyme reaction products, with trans-esterification reactions of vegetable oils. They have evaluated the correlation capacity of these data using the cubic equation of state of PR with van der Waals mixing rules with two binary interaction parameters to describe the phase equilibrium of those systems. The PR equation accurately represents the systems studied.

Oliveira *et al.* [12] used the equation CPA (Cubic-Plus-Association) developed by Soave-Redlich-Kwong (SRK) in association with a term proposed by Wertheim to predict the solubility of water in different methyl esters. In fact, it reveals a good prediction of vapor-liquid equilibrium data, with deviations below 1%. According to the authors, the average deviation for predicting the solubility of water in ethers was less than 7%, while for predicting biodiesel, using the ester-mixing rule (biodiesel as a pseudo-component), the average deviation was around 16%. This study has been extended to the ternary systems containing methanol + glycerol + methyl oleate (as principal constituents of soybean oil biodiesel). Good results have been found in the prediction of the liquid-liquid equilibrium, thanks to the optimization of the binary interaction parameters.

Shimoyama *et al.* [13] used the equation of PR Stryjet-Vera (PR-SV) to predict the vapor-liquid equilibrium of glycerol + ethanol and glycerol + methanol systems, using a rule of conventional mixture (quadratic) and a rule of mixture proposed by PRASOG (Peng-Robinson group contribution method). The equation PR-SV represented well the compositions of the liquid phase when the quadratic mixing rule was used, but the best results for the vapor phase were found using the mixing rule proposed by PRASOG.

Cheng *et al.* [16] used the UNIQUAC model to represent the liquid-liquid phase equilibrium of the methanol + triglyceride + methyl oleate system at temperatures of 293, 313 and 333 K at atmospheric pressure. The model gave consistent results with the measured experimental results.

Huber *et al.* [10] proposed a Helmholtz-type equation for modeling the thermodynamic properties of biodiesel from the mixture of five methyl esters that make soybean biodiesel (methyl palmitate, methyl oleate, methyl stearate, methyl linoleate and methyl linolenate). The density, speed of sound, and boiling point data at 83 kPa were compared with the properties obtained by the model. The authors indicated that the model could represent the thermodynamic properties of any biodiesel that may have the composition expressed in the esters mentioned above. The average deviations noted by the authors are 0.6% for density prediction, 0.4% for the speed of sound and boiling temperature.



Ndiaye et al. [17] studied the behavior of soybean and castor oils and their ethyl esters in equilibrium with carbon dioxide at high pressures. The authors used the PR and SAFT (Statistical Associating Fluid Theory) equations to represent the experimental data. For fatty acid esters (biodiesel components), the PR equation and the SAFT equation represented the experimental data, whereas for oils, the SAFT equation was better.

M'Hamdi Alaoui et al. [18] have studied the liquid density of mixtures of biofuels for the system 1-heptanol + heptane at pressures up to 140 MPa and temperatures between 298.15 K and 393.15 K, the data of the experimental density have been predicted with Tait (EoS) with low standard deviations less than 0.06%. The excess volumes have been calculated from the experimental data. In addition, thermo-physical properties such as the isobaric thermal expansivity and isothermal compressibility were derived from the Tait equation.

In this work, experimental densities of fatty acid methyl esters (FAME) were compiled from the literature [5-9], especially for Methyl laurate (12:0), Methyl myristate (14:0), Methyl palmitate (16:0), Methyl stearate (18:0), Methyl oleate (18:1), Methyl linoleate (18:2) and Methyl linolenate (18:3) over the temperature range between 270 K - 393.15 K and pressures between 0.1 MPa - 80 MPa. Experimental density data were correlated by three equations of state: PR, Tait and PC-SAFT. For PR EoS, we adopted a synthesis approach of previous studies to select the critical parameters. However, for the Tait equation, the characteristic coefficients for each methyl ester were determined by fitting the equation to the experimental data, and for the PC-SAFT equation, the characteristic parameters related to FAME were estimated by adjusting the equation to the experimental data. In addition, the isobaric thermal expansivity and isothermal compressibility were derived from the Tait equation for each fatty acid methyl ester.

2. Correlation and Modeling

2.1. Databank

The experimental density data (448 points) reported in this work are accumulated and selected from the literature [5-9]. Table 1 summarizes the references, the names and the chemical formula of each compound (FAME), in addition, the number of experimental points (N_{exp}) and the pressure and temperature ranges.

Table 1: Database for Experimental FAME Density

| Reference | FAME | FAME names | FAME formula | M (g/mol) | N_{exp} | Temperature range (K) | Pressure range (MPa) |
|-----------|---------|-------------------|-------------------|-----------|-----------|-----------------------|----------------------|
| [5] | C(12:0) | Methyl laurate | $C_{13}H_{26}O_2$ | 214.35 | 83 | [283.15-333.15] | [0.1-45] |
| [6] | C(14:0) | Methyl myristate | $C_{15}H_{30}O_2$ | 242.40 | 89 | [303.15-393.15] | [0.1-80] |
| [6] | C(16:0) | Methyl palmitate | $C_{17}H_{34}O_2$ | 270.45 | 47 | [313.15-383.15] | [0.1-50] |
| [7] | C(18:0) | Methyl stearate | $C_{19}H_{38}O_2$ | 298.51 | 10 | [313.15-363.15] | [0.1] |
| [8] | C(18:1) | Methyl oleate | $C_{19}H_{36}O_2$ | 296.49 | 83 | [270-390] | [0.1-50] |
| [8] | C(18:2) | Methyl linoleate | $C_{19}H_{34}O_2$ | 294.48 | 83 | [270-390] | [0.1-50] |
| [9] | C(18:3) | Methyl linolenate | $C_{19}H_{32}O_2$ | 292.46 | 83 | [273.15-363.15] | [0.1] |

2.2. Empirical Models:

2.2.1 Peng-Robinson (PR) equation

The information concerning the cubic PR EoS presented in equation (1) is available in the literature [19]. The intention of choosing a cubic equation of state was to be able to represent the pVT (pressure-volume-temperature) behavior of the liquid and vapor biodiesel in a wide range of temperature and pressure with only three parameters, thus, adding its simplicity and its generality. With the parameters of this equation, it is possible to predict the fugacity coefficient of FAME and the other thermodynamic properties. The PR equation is well documented and its formulation is presented as follows:



$$Z = \frac{1}{1-b\rho} - \frac{a}{\rho RT \left(\frac{1}{\rho^2} + \frac{2b}{\rho} - \frac{1}{b^2} \right)} \quad (1)$$

Where a and b are defined as:

$$a_i = 0,45724 \frac{R^2 T_{ci}^2}{P_{ci}} \left[1 - \left(0,37464 + 1,54226\omega_i - 0,266992\omega_i^2 \right) \left(1 - \frac{T}{T_{ci}} \right)^{1/2} \right]^2 \quad (2)$$

$$b_i = 0,0778 \frac{RT_c}{P_c} \quad (3)$$

T_c and p_c represent the temperature and the critical pressure respectively, the dependence of parameter (a) with temperature introduces a new parameter into the PR equation, the acentric factor (ω). This dependency has been added to the equation to make it possible to reproduce the vapor pressure of the hydrocarbons with the equation of state [20].

To use the PR equation, it is necessary to obtain experimental critical data for long-chain ester molecules. These molecules that make biodiesel submit a thermal degradation before the critical point is obtained experimentally [21]. Several works have predicted the critical properties of pure substances as fatty acid methyl esters [20, 22-24].

The performance of the equation of PR has been evaluated by calculating the absolute average deviation (AAD) defined as follows:

$$AAD = \frac{100}{N} \sum_{i=1}^N \left| \frac{\rho_i^{\text{exp}} - \rho_i^{\text{calc}}}{\rho_i^{\text{exp}}} \right| \quad (4)$$

2.2.2 PC-SAFT equation

The PC-SAFT equation, as well as the SAFT equation, developed by Chapman et al. [25] is based on statistical thermodynamics. The PC-SAFT equation proposed by Gross and Sadowski [26] for complex fluids is a modification of the SAFT equation. The general equation of PC-SAFT is written as a sum of three terms of residual Helmholtz energy that reflects different contributions of the intermolecular forces present in the molecule: the first term is relating to the hard chain part, the second one to the dispersion part and the third to the association. The equation presented in this work contains only two terms of the general equation. The PC-SAFT equation can be expressed in terms of residual Helmholtz energy for mixtures of non-associative molecules according to the equation (5).

$$\bar{a}^{\text{res}} = \bar{a}^{\text{hc}} + \bar{a}^{\text{disp}} \quad (5)$$

Where, \bar{a}^{hc} , is the contribution of the hard chain reference system and, \bar{a}^{disp} , is the contribution of the dispersion force, The contribution of the hard chain reference system was provided and defined by Gross and Sadowski. It depends on the average number of segments, \bar{m} , and on the distribution of radial pairs of segments, \bar{g}_{ij}^{hs} , as can be seen in equation (6)

$$\bar{a}^{\text{hc}} = \bar{m} \bar{a}^{\text{hc}} - \sum_{i=1}^{n_c} (m_i - 1) \ln g_{ij}^{\text{hs}} \quad (6)$$

The dispersion term, \bar{a}^{disp} , explains the Van der Waals forces between different segments. In this work, we use the dispersion expression defined by Gross and Sadowski. This expression is presented as follows:

$$\bar{a}^{\text{disp}} = -2\pi \bar{\rho} I_1 m^2 \varepsilon \sigma^3 - \pi \bar{\rho} m C_1 I_2 m^2 \varepsilon^2 \sigma^3 \quad (7)$$



Where the coefficient C_1 depends on the number of segments (\bar{m}) and the reduced density $\check{\rho}$; the perturbation integrals I_1 and I_2 are expressed also by the reduced density $\check{\rho}$ and represent the parameters of size and pair energy of segments, respectively.

PC-SAFT parameters were estimated by fitting the PC-SAFT equations to the experimental density presented in this work. The parameters were determined by minimizing the following objective function (Obj.F):

$$Obj.F = \sum_{i=1}^N \left(\frac{\rho_i^{\text{exp}} - \rho_i^{\text{calc}}}{\rho_i^{\text{exp}}} \right)^2 \quad (8)$$

Where N represents the number of data points. ρ_i^{exp} and ρ_i^{calc} Represent the experimental and calculated densities, respectively.

2.2.3. Tait equation

Density data at different temperatures and pressures were fitted to Tait EoS [27]. This equation is a simple and fast way to obtain derived thermodynamic properties, such as isothermal compressibility, isobaric expansivity from experimental data of p , ρ and T . The empirical Tait EoS has been used since the end of the 19th century to adjust the high pressure density of all types of liquids, high molecular weight polymers and even compressibility data for solids and molten salts [28-30]. The Tait EoS has the following expression:

$$\rho(T,p) = \frac{\rho_0(T,0.1\text{MPa})}{1 - C \ln \left(\frac{B(T) + p}{B(T) + 0.1\text{MPa}} \right)} \quad (9)$$

Where ρ is the molar density, p , the pressure, T , the temperature, $(T, P_{\text{ref}}(T))$ is the dependence of the density with the temperature at the reference pressure, normally at atmospheric pressure or saturation. For this work, the atmospheric pressure was taken as the reference pressure. This function $\rho_0(T, p=0.1\text{MPa})$ has the following form:

$$\rho_0(T) = A_0 + A_1T + A_2T^2 \quad (10)$$

Where, the coefficients A_i are determined from the experimental results of the density at atmospheric pressure. The denominator of equation (9) changes with temperature and pressure. The parameter C is considered independent of the temperature and for $B(T)$, the following polynomial expression has been used:

$$B(T) = B_0 + B_1T + B_2T^2 \quad (11)$$

The experimental values of the density can be derived to obtain important quantities such as isothermal compressibility, κ_T , expressed as follows.

$$\kappa_T = \left(\frac{1}{\rho} \right) \left(\frac{\partial \rho}{\partial p} \right)_T = \frac{C}{\left(1 - C \ln \left(\frac{B(T) + p}{B(T) + 0.1\text{MPa}} \right) \right) (B(T) + p)} \quad (12)$$

Or isobaric thermal expansivity, α_p , expressed by equation (13)

$$\alpha_p = - \left(\frac{1}{\rho} \right) \left(\frac{\partial \rho}{\partial T} \right)_p \quad (13)$$

Some authors [31] and [32] note that the isobaric expansivity depends on both functions $B(T)$ and $\rho_0(T)$; In the same way, they report that the differences which can sometimes be found for α_p values in the literature compared to



experimental values are due to the difference in density values, and also due to the adjustment equations used. In this way, it is proposed to derive the isobaric expansivity from the isobaric densities. Thus, at each pressure we can assume that:

$$\rho_p(T) = a_0 + a_1T + a_2T^2 \quad (14)$$

Therefore:

$$(\partial\rho/\partial T)_p = a_1 + 2a_2T \quad (15)$$

For each pressure, a set of values (a_0 , a_1 , a_2) are obtained by means of a least squares adjustment. Inserting the differentiated density $\rho_p(T)$ and the densities calculated in equation (14) we arrive at the isobaric expansivity expression:

$$\alpha_p = -\frac{a_1 + 2a_2T}{a_0 + a_1T + a_2T^2} \quad (16)$$

The estimated uncertainty is $\pm 1\%$ for the isothermal compressibility, and around $\pm 3\%$ for the isobaric thermal expansivity.

The performance of the Tait equation was evaluated by calculating the absolute average deviation (AAD), the maximum deviation (MD), the average deviation (Bias) and the standard deviation (σ) which are defined as follows:

$$\text{AAD} = \frac{100}{N} \sum_{i=1}^N \left| \frac{\rho_i^{\text{exp}} - \rho_i^{\text{calc}}}{\rho_i^{\text{exp}}} \right| \quad (17)$$

$$\text{MD} = \text{Max} \left(100 \left| \frac{\rho_i^{\text{exp}} - \rho_i^{\text{calc}}}{\rho_i^{\text{exp}}} \right| \right) \quad (18)$$

$$\text{Bias} = \frac{100}{N} \sum_{i=1}^N \frac{\rho_i^{\text{exp}} - \rho_i^{\text{calc}}}{\rho_i^{\text{exp}}} \quad (19)$$

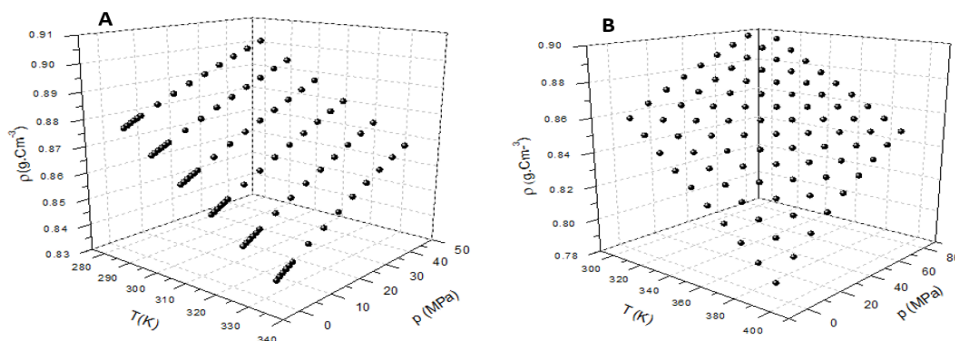
$$\sigma = \sqrt{\frac{\sum_{i=1}^N (\rho_i^{\text{exp}} - \rho_i^{\text{calc}})^2}{N-m}} \quad (20)$$

Where, N, is the number of experimental data and, m, is the number of parameters ($m = 8$).

3. Results & Discussion

3.1. Density

Several density data of FAME are available in the literature at various temperatures and pressures. The densities of FAME were compiled under temperature conditions between 270 K and 393.15 K and at pressures up to 80 MPa. Experimental density data (448 points) reported in this work are presented as a function of temperature and pressure in Figure 1 (from (a) to (e)).



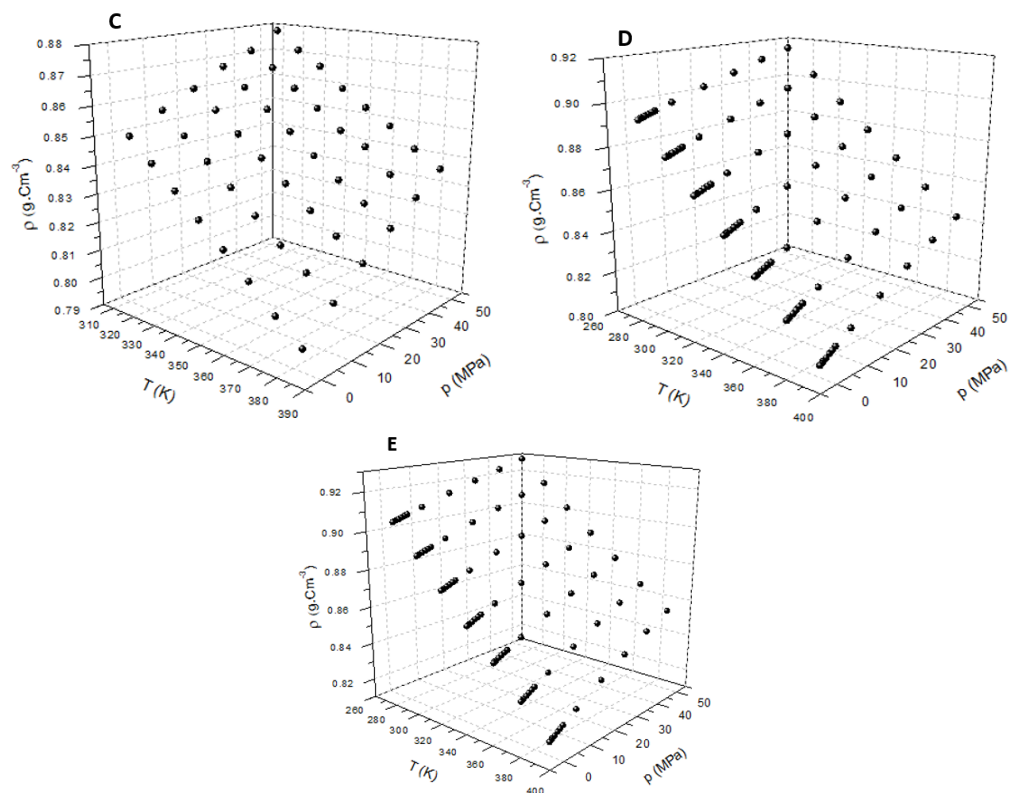


Figure 1: Experimental densities of studied FAME as a function of pressures and temperatures: A: Methyl laurate (12:0); B: Methyl myristate (14:0); C: Methyl palmitate (16:0); D: Methyl oleate (18:1); and E: Methyl linoleate (18:2).

To our knowledge, the density data for several pressures (except atmospheric pressure) for FAME (18: 0) and (18: 3) are not available in the literature. As expected, the density of FAME decreases with temperature and increases when the pressure increases at a constant temperature. Due to the increase of kinetic energy, the temperature rises and causes a strong movement of molecules. As a result, the molecular weight per unit volume decreases, thus, the density drops with temperature.

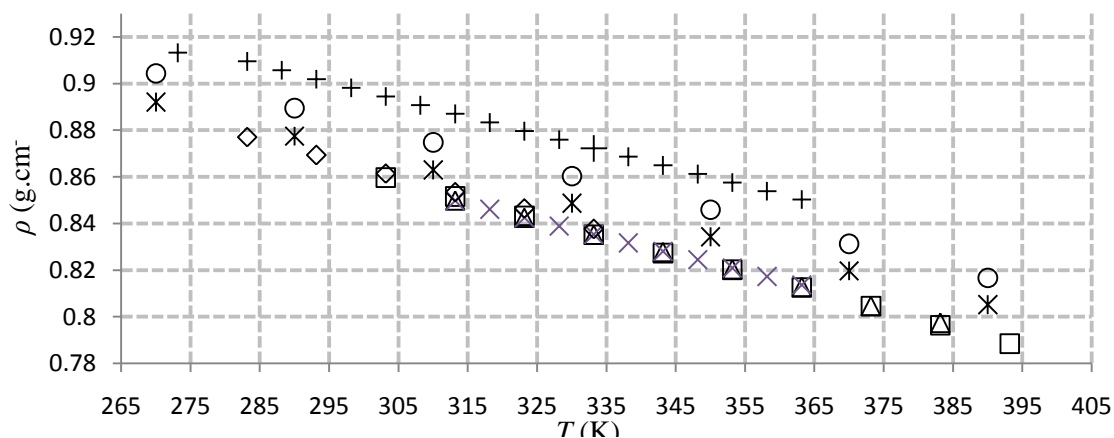


Figure 2: Experimental densities of studied FAME as a function temperatures at atmospheric pressure: \diamond : Methyl laurate (12:0); \square : Methyl myristate (14:0); Δ : Methyl palmitate (16:0); \times : Methyl stearate (18:0); \star : Methyl oleate (18:1); \star : Methyl linoleate (18:2); $+$: Methyl linolenate (18:3)



Figure 2 shows the density variation for the methyl esters. An opposite effect of density vs molecular weight was observed. i.e. The density decrease proportionally with increasing molecular weight: $\rho(\text{C18: 0}) > \rho(\text{C16: 0}) > \rho(\text{C14: 0}) > \rho(\text{C12: 0})$. On the other hand, the densities of FAME are proportional to the number of double bonds at atmospheric pressure (for example: $\rho(\text{C18: 3}) > \rho(\text{C18: 2}) > \rho(\text{C18: 1}) > \rho(\text{C18: 0})$).

3.1.1. Tait equation results

Figures 3 and 4 show the capability to reproduce the experimental density of FAME. They describe the comparison between the experimental data and the results predicted by the Tait and PC-SAFT equations, as a function of pressure and the temperature at atmospheric pressure, respectively.

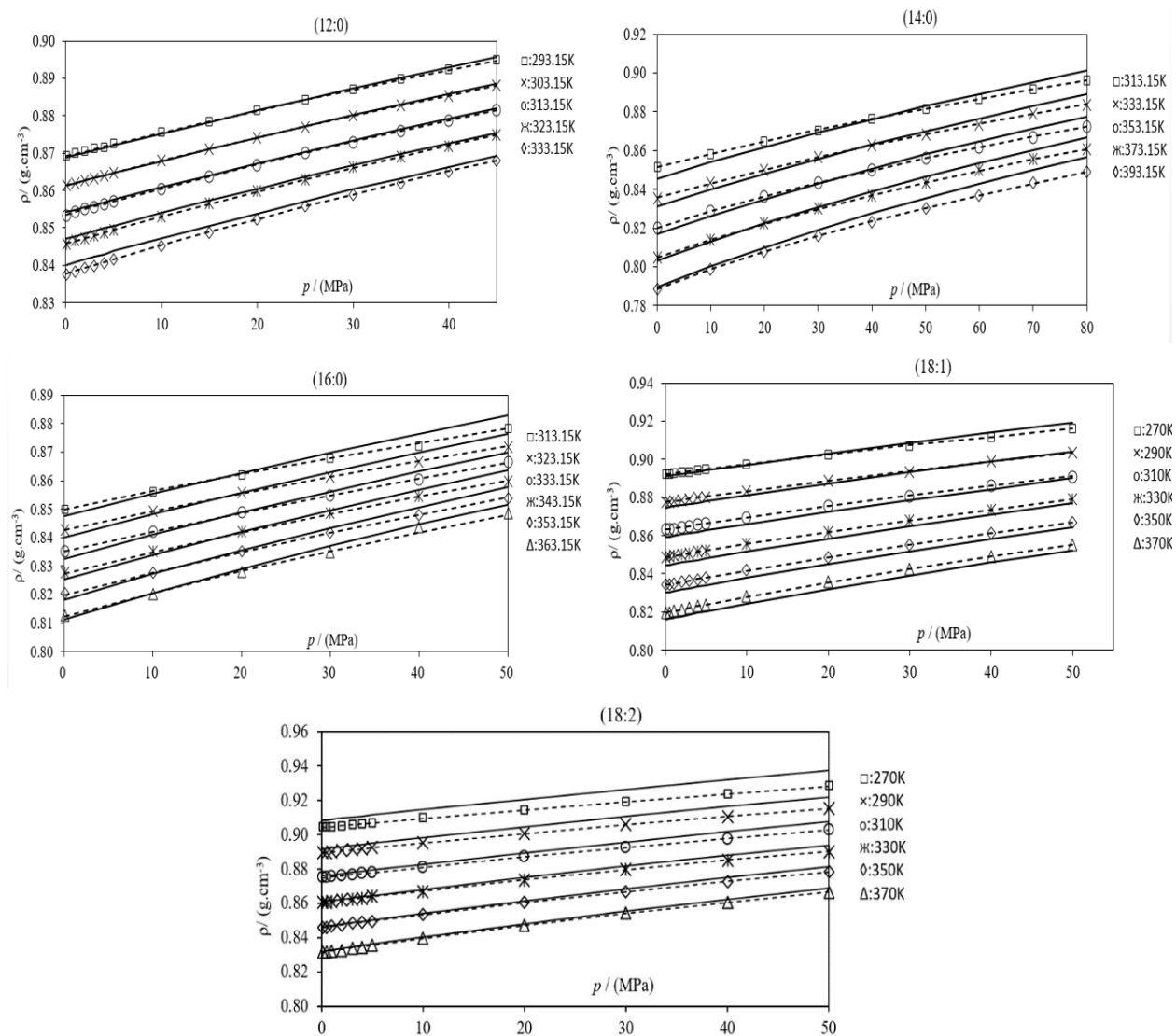


Figure 3: Comparison of experimental density data (symbols) for FAME relative to those calculated by (—) PC-SAFT and (---) Tait equations as a function of pressure at several temperatures.

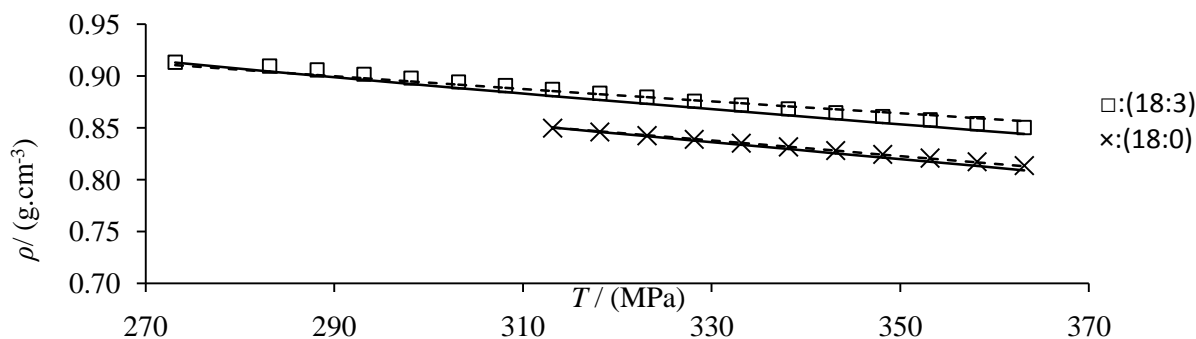


Figure 4: Comparison of experimental density data (symbols) for Methyl stearate (18:0) and Methyl linolenate (18:3) relatives to those calculated by (—) PC-SAFT and (---) Tait equations as a function of temperatures at atmospheric pressure

The coefficients of the Tait equation for each FAME, as well as MD, bias and standard deviation, σ , are listed in Table 2. In order to compare the predicted densities obtained in this work with previous publications results, the average absolute deviation (AAD) was calculated for multiple articles. The results showed reasonable accuracy according to literature, with a low average deviation. In fact, the value of AAD for methyl laurate is equal to 0.009% closed to 0.008% found by Pratas et al [5]. In addition, The AAD of methyl myristate obtained is 0.006%, exactly the same value compared to Pratas et al [5] work but inferior to the AAD found in Ndiaye et al [6] publication. According to Pratas et al [5], The AAD of methyl oleate is 0.003% well below 0.01% determined in the present work. Besides, for methyl palmitate, the AAD calculated is 0.03%, slightly below 0.052% based on Ndiaye et al [6] work. For methyl linoleate and methyl setearate, the AAD is respectively 0.01% and 0.04%. In contrast, the highest proportion of AAD observed is for methyl linolenate with a percentage of 0.35%. Overall, we can summarize that all the studied components show a low average of AAD except methyl linolenate with the highest percentage.

Table 2: Obtained parameters and deviations for density predicted by Tait equation of FAME

| | 12:0 | 14:0 | 16:0 | 18:0 | 18:1 | 18:2 | 18:3 |
|---|-----------------------|-----------------------|-----------------------|------------------------|------------------------|-----------------------|------------------------|
| $A_0 / \text{g} \cdot \text{cm}^{-3}$ | 1.696 | 1.651 | 0.727 | 0.727 | 1.111 | 1.15 | 1.15 |
| $A_1 / \text{g} \cdot \text{cm}^{-3} \cdot \text{K}^{-1}$ | $-6.65 \cdot 10^{-3}$ | $-5.57 \cdot 10^{-3}$ | $2.40 \cdot 10^{-3}$ | $2.40 \cdot 10^{-3}$ | $-9.36 \cdot 10^{-4}$ | $-1.17 \cdot 10^{-3}$ | $-1.17 \cdot 10^{-3}$ |
| $A_2 / \text{g} \cdot \text{cm}^{-3} \cdot \text{K}^{-2}$ | $1.92 \cdot 10^{-5}$ | $1.37 \cdot 10^{-5}$ | $-9.21 \cdot 10^{-6}$ | $-9.21 \cdot 10^{-6}$ | $6.42 \cdot 10^{-7}$ | $1.28 \cdot 10^{-6}$ | $1.28 \cdot 10^{-6}$ |
| $A_3 / \text{g} \cdot \text{cm}^{-3} \cdot \text{K}^{-3}$ | $-2.09 \cdot 10^{-8}$ | $-1.31 \cdot 10^{-8}$ | $8.96 \cdot 10^{-9}$ | $8.97 \cdot 10^{-9}$ | $-6.47 \cdot 10^{-10}$ | $-1.22 \cdot 10^{-9}$ | $-7.99 \cdot 10^{-10}$ |
| B_0 / MPa | 443.8 | 434.6 | 585.7 | 585.7 | 408.9 | 412.8 | 412.8 |
| $B_1 / \text{MPa} \cdot \text{K}^{-1}$ | -1.489 | -1.485 | -2.214 | -2.214 | -1.367 | -1.371 | -1.371 |
| $B_2 / \text{MPa} \cdot \text{K}^{-2}$ | $1.34 \cdot 10^{-3}$ | $1.39 \cdot 10^{-3}$ | $2.31 \cdot 10^{-3}$ | $2.31 \cdot 10^{-3}$ | $1.25 \cdot 10^{-3}$ | $1.26 \cdot 10^{-3}$ | $1.26 \cdot 10^{-3}$ |
| C | 0.09143 | 0.08853 | 0.09193 | 0.09193 | 0.08118 | 0.08151 | 0.08151 |
| $\sigma / \text{g} \cdot \text{cm}^{-3}$ | $7.89 \cdot 10^{-5}$ | $6.45 \cdot 10^{-5}$ | $2.46 \cdot 10^{-4}$ | $1.26 \cdot 10^{-4}$ | $1.11 \cdot 10^{-4}$ | $9.57 \cdot 10^{-5}$ | $1.33 \cdot 10^{-3}$ |
| AAD / % | 0.009 | 0.006 | 0.03 | 0.04 | 0.01 | 0.01 | 0.35 |
| MD / % | 0.03 | 0.05 | 0.23 | 0.08 | 0.03 | 0.03 | 0.74 |
| Bias / % | $-9.94 \cdot 10^{-7}$ | $2.73 \cdot 10^{-14}$ | $-9.88 \cdot 10^{-7}$ | $-4.07 \cdot 10^{-14}$ | $-2.53 \cdot 10^{-15}$ | $-9.93 \cdot 10^{-7}$ | $-1.00 \cdot 10^{-6}$ |

Figure 5 illustrates the deviations vs. pressures between the experimental data for the studied FAME relatives to those calculated from Tait equation for each FAME as a function of pressure, with the exception of (18:0) and (18:3) which were illustrated as a function of temperature at atmospheric pressure in Figure 6.



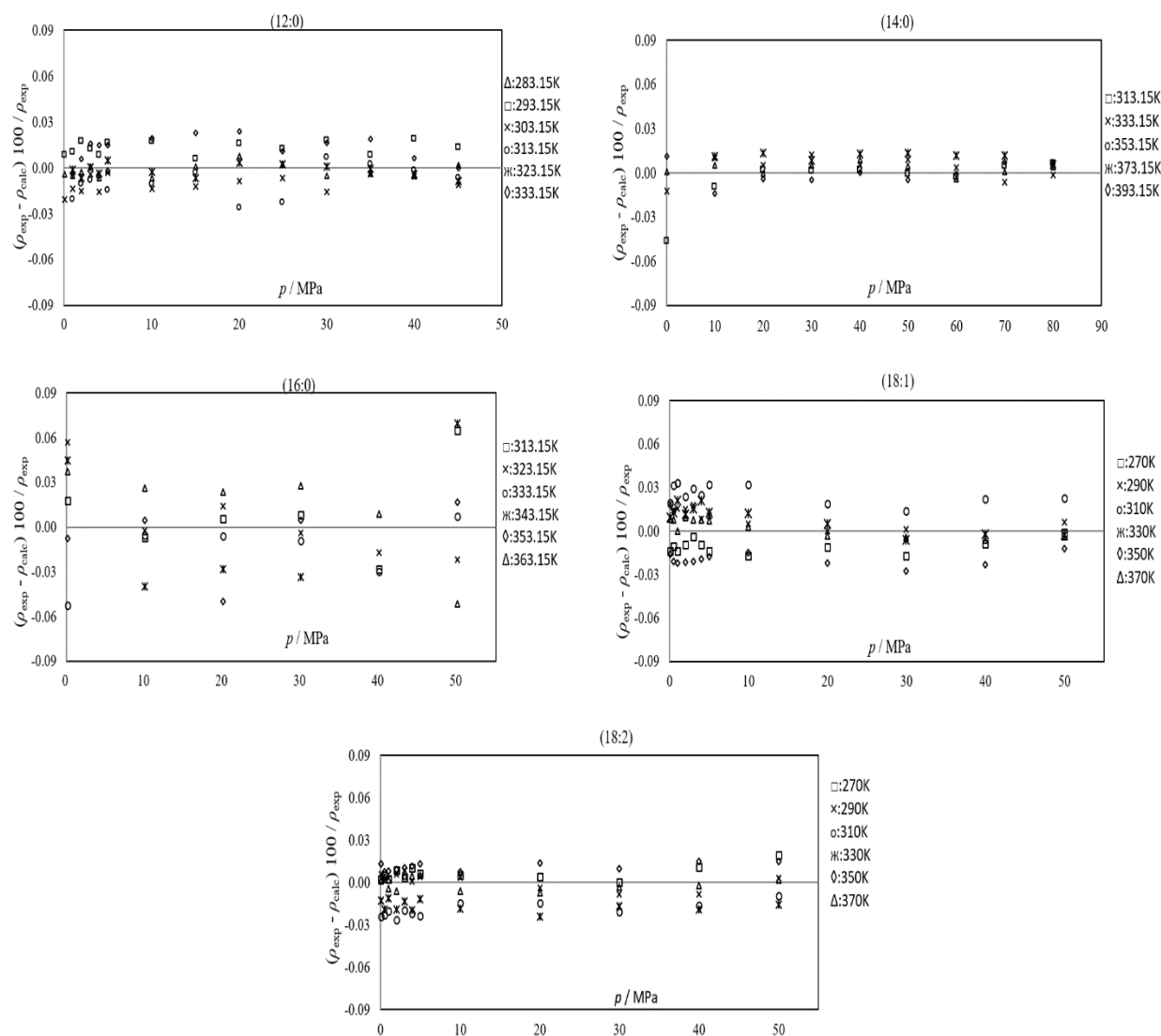


Figure 5: Deviations vs. pressures for the studied FAME relative to those calculated from Tait equation

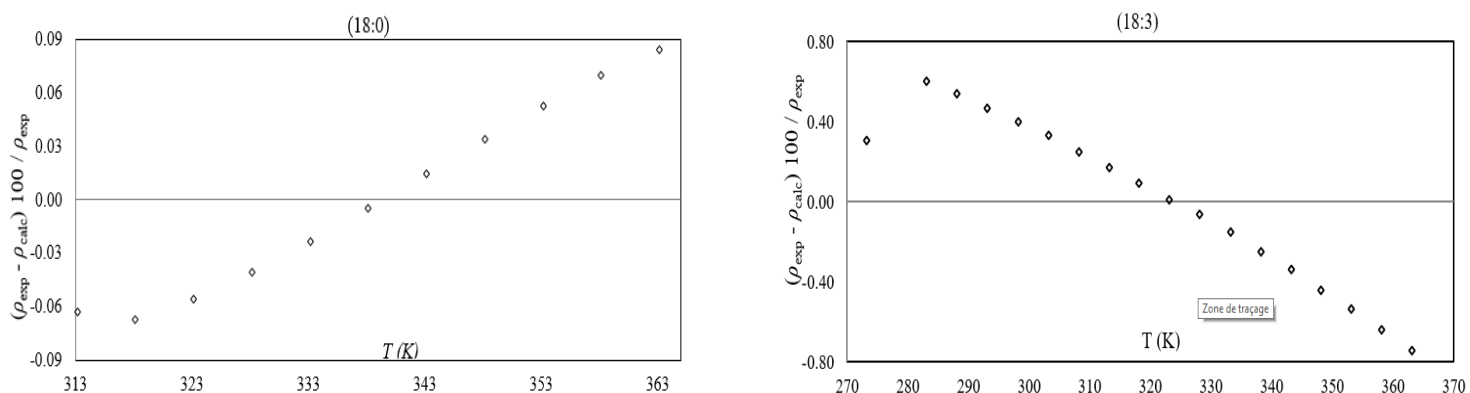


Figure 6: Deviations vs. temperatures for Methyl stearate (18:0) and Methyl linolenate (18:3) relative to those calculated from Tait equation

A good agreement is observed, the maximum standard deviation is noted for methyl linolenate with $\sigma = 1.33 \cdot 10^{-3} \text{ g} \cdot \text{cm}^{-3}$ at low pressure, the variation of the density as a function of temperature is non-linear, because the temperature range considered here is sufficiently large, which makes the use of equation (9) reliable. Moreover, the non-linear form of the Tait-like equation makes the representation of the behavior of density in relation to the pressure. The absolute deviations (%) between the experimental data and the predicted densities are summarized as follows: $1.5 \cdot 10^{-4} \leq (12:0) \leq 2.6 \cdot 10^{-2}$; $6.7 \cdot 10^{-5} \leq (14:0) \leq 4.6 \cdot 10^{-2}$; $2.4 \cdot 10^{-3} \leq (16:0) \leq 0.23$; $5 \cdot 10^{-3} \leq (18:0) \leq 8.4 \cdot 10^{-2}$; $1.3 \cdot 10^{-6} \leq (18:1) \leq 3.3 \cdot 10^{-2}$; $2.6 \cdot 10^{-4} \leq (18:2) \leq 2.7 \cdot 10^{-2}$ and $1.1 \cdot 10^{-2} \leq (18:3) \leq 0.74$.

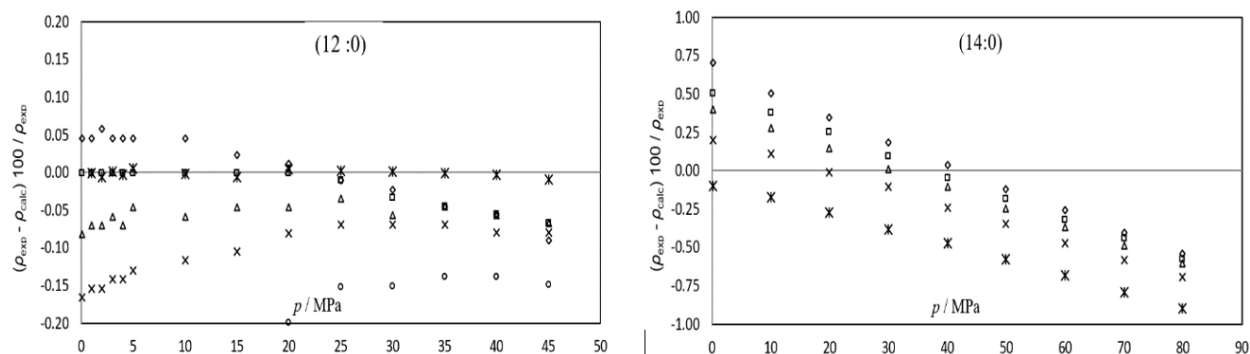
3.1.2. PC-SAFT equation results

The comparison between the experimental data and the results correlated by the PC-SAFT equation are illustrated in Figures 3 and 4. The PC-SAFT parameters and the average absolute deviation (AAD) for each FAME are listed in Table 3.

Table 3: Characteristic parameters of PC-SAFT model of FAMES:

| FAME | MW [g.mol ⁻¹] | <i>m</i> [-] | σ [Å] | <i>k</i> [K] | AAD % ($\frac{1}{p}$) |
|------|------------------------------|-----------------|--------------|-----------------|----------------------------|
| 12:0 | 214.35 | 6.9470 | 3.7242 | 297.35 | 0.01 |
| 14:0 | 242.402 | 7.4190 | 3.7799 | 269.61 | 0.3 |
| 16:0 | 270.456 | 9.50 | 3.6003 | 253.2952 | 0.2 |
| 18:0 | 298.510 | 10.9387 | 3.5017 | 218.2502 | 0.001 |
| 18:1 | 296.494 | 11.9615 | 3.4315 | 250.6074 | 0.4 |
| 18:2 | 294.478 | 11.6435 | 3.4315 | 250.6074 | 0.06 |
| 18:3 | 292.462 | 10.8387 | 3.5024 | 257.2502 | 0.005 |

The density values correlated by the PC-SAFT equation as a function of pressure and temperature show a good agreement compared to the experimental data for (18: 0) with AAD = 0.001%, (18: 3) with AAD = 0.005%, (12: 0) and (18: 2) with AAD = 0.01 and 0.06% respectively. Moreover, we can conclude that generally all the studied components show a low average of AAD comparing with the AAD data reported by Dong et al [4] except methyl oleate. Figure 7 illustrates the deviations vs. pressures between the experimental data for the studied FAME relatives to those calculated from PC-SAFT equation, except (18: 0) and (18: 3) which were illustrated as a function of temperature in Figure 8.



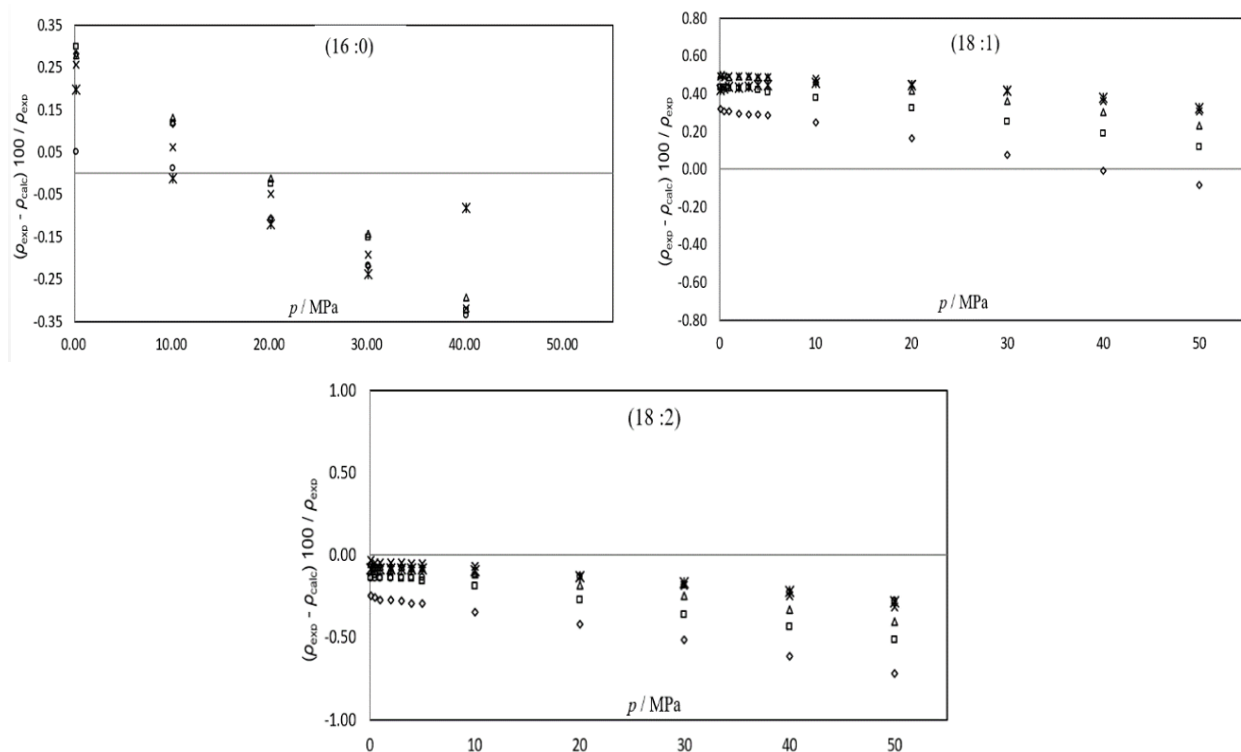


Figure 7: Deviations vs. pressures for the studied FAMEs relative to those calculated from PC-SAFT equation. Symbols as in Fig. 5.

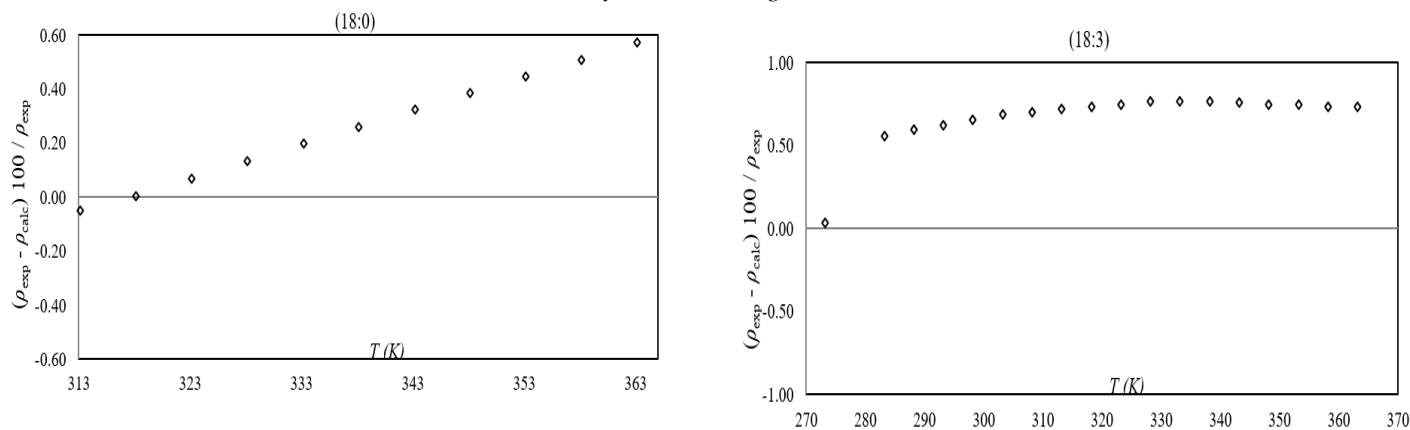


Figure 8: Deviations vs. temperature for the studied FAMEs relative to those calculated from PC-SAFT equation

A good agreement is observed. The absolute deviations (%) between the experimental data and the correlated densities are summarized as follows: $1.9 \cdot 10^{-3} \leq (12:0) \leq 9.4 \cdot 10^{-1}$, $1.1 \cdot 10^{-2} \leq (14:0) \leq 8.9 \cdot 10^{-1}$, $1 \cdot 10^{-2} \leq (16:0) \leq 5.7 \cdot 10^{-1}$, $4 \cdot 10^{-3} \leq (18:0) \leq 5.7 \cdot 10^{-1}$, $3 \cdot 10^{-2} \leq (18:1) \leq 5.5 \cdot 10^{-1}$; $4 \cdot 10^{-2} \leq (18:2) \leq 1$ and $4 \cdot 10^{-2} \leq (18:3) \leq 0.76$. It is important to note that the high deviation showed (0.2, 0.3 and 0.4%) were probably not related to the PC-SAFT equation applied in this work, as some authors have shown that this equation can correlate density with accuracy for many classes of compounds, including esters [33-36]. In general, the densities correlated by the PC-SAFT equation show good agreement for FAME compared to experimental data.

3.1.3. PR equation results

Due to the thermal decomposition of FAME, the critical properties T_c , p_c , and ω are not known from experimental sources. Some methods are proposed to estimate these properties using group contribution methods. For the use of

the PR equation, the T_c , p_c and acentric factors, ω , parameters were selected using a comparative bibliographic study [37-41]. Density calculations were performed by Matlab®. Table 4 summarizes the source and values of these three parameters, thus the AAD found for each compound (FAME) by comparing the experimental and calculated density, and the figures 9 show a comparison of experimental density data relative to those calculated by PR EoS as a function of pressure at several temperatures.

Table 4: Critical Parameters of Studied FAME:

| FAME | MW[g.mol ⁻¹] | T _c (K) | P _c (bar) | ω | AAD (%) |
|--------|--------------------------|-----------------------|-------------------------|------------------------|---------|
| (12:0) | 214.35 | 712 ^[38] | 19.9604 ^[39] | 0.6319 ^[39] | 0.75 |
| (14:0) | 242.402 | 718 ^[39] | 17.4323 ^[39] | 0.7035 ^[39] | 1.23 |
| (16:0) | 270.456 | 765 ^[38] | 16.4285 ^[39] | 0.8767 ^[39] | 1.01 |
| (18:0) | 298.510 | 774 ^[36] | 13.9071 ^[39] | 1.0000 ^[35] | 6.85 |
| (18:1) | 296.494 | 772 ^[37] | 13.8132 ^[39] | 1.0000 ^[35] | 9.75 |
| (18:2) | 294.478 | 795 ^[37] | 13.8132 ^[39] | 1.0000 ^[35] | 13.9 |
| (18:3) | 292.462 | 797.3 ^[38] | 13.0170 ^[38] | 0.9770 ^[36] | 21.0 |

□ reference of critical parameters

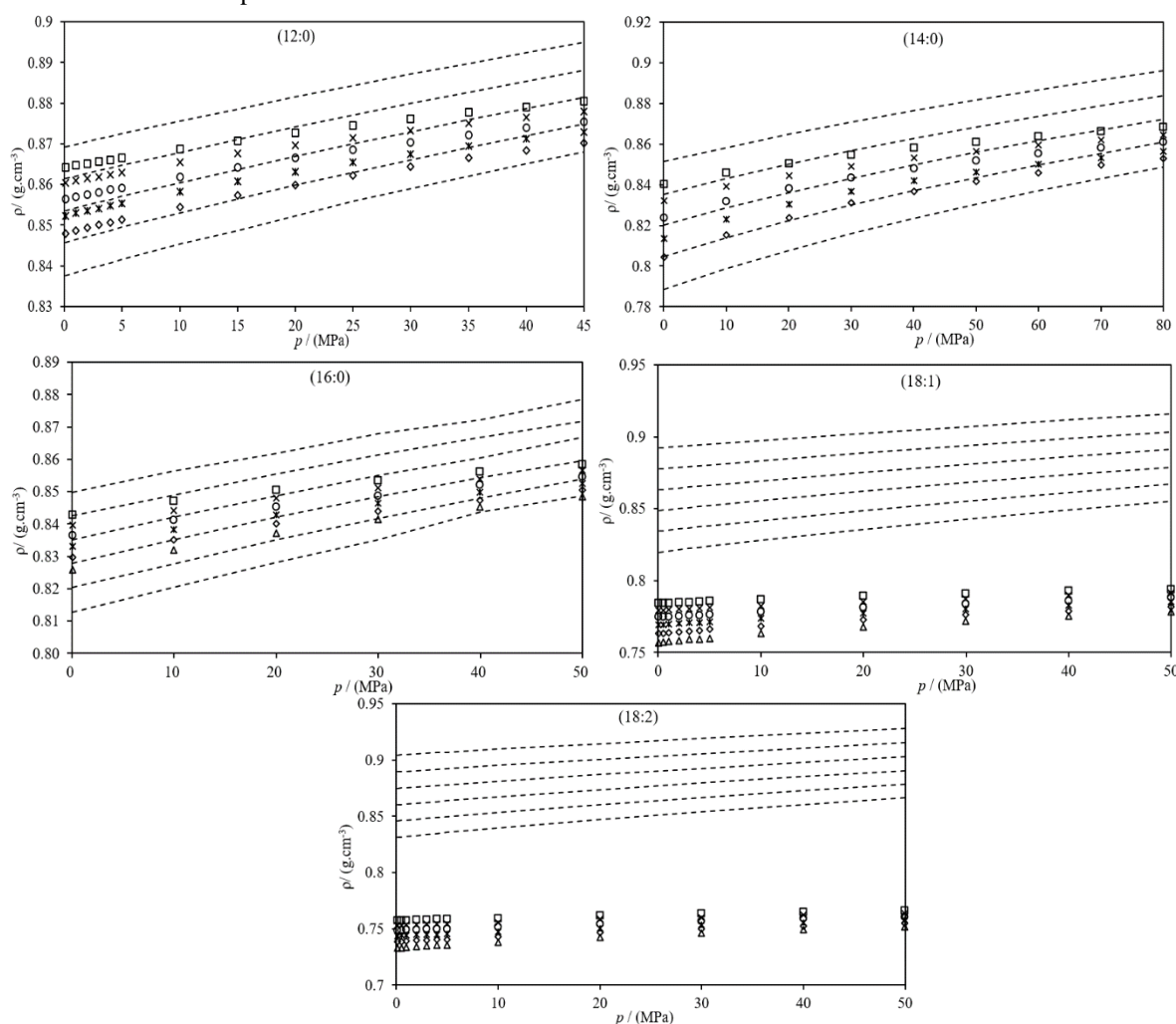


Figure 9: Comparison of experimental density data (---) for FAMES relative to those calculated by PR EoS (symbols) as a function of pressure at several temperatures. Symbols as in Figure 3.

Cubic EoS is probably the most widely used for engineering applications and, for this reason, many modifications have been proposed. Thus, in order to improve the cubic EoS, various functional terms or additional parameters



have been proposed which allows better calculations of liquid densities. However, despite the success of cubic EoS, the accuracy of these equations decreases when predicting the behavior of substances that form strong associations between molecules, such as hydrogen bonding or long-chain complex fluids with double bonding interactions, because classical EoS have been developed in considering only the attractive forces for dispersion. Generally, the results of AAD obtained was higher for all FAME using the PR as cubic EoS. Therefore, PR EoS is not appropriate for predicting the density of long-chain compounds. We claim that the methodologies that use cubic equations of state must be not safe for the evaluation of complex fluids, because these equations do not present good results for polar, associating and/or large molecules [42].

3.2. The derived thermodynamic properties

The derived thermodynamic properties, such as isothermal compressibility, κ_T , and isobaric thermal expansivity, α_p , are calculated from the Tait equation. Generally, κ_T and α_p can be obtained from the partial derivatives of density as a function of pressure or temperature (see eq (12) and (13): $\kappa_T = (1/\rho) (\partial\rho/\partial p)_T$, $\alpha_p = - (1/\rho) (\partial\rho/\partial T)_p$). These properties are used to provide more specific information on the dependence of fluid density at temperature as a function of temperature and pressure. Figures 10 and 11 show, respectively, the variation of the isothermal compressibilities, κ_T , and isobaric thermal expansivity, α_p of FAME ((12:0), (14:0), (16:0), (18:1) and (18:2)) as a function of pressure at available temperatures.

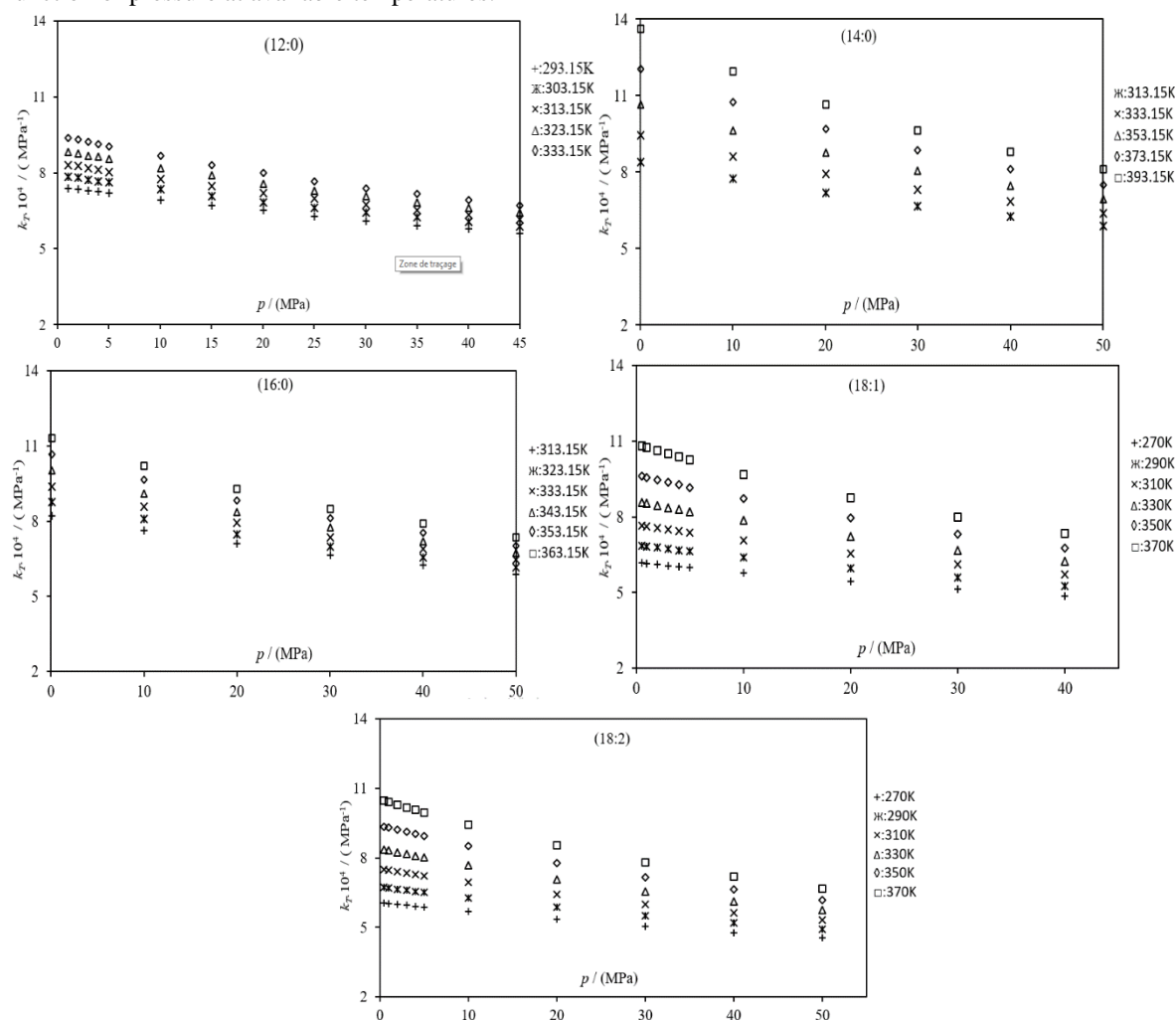


Figure 10: Isothermal compressibility, κ_T , calculated from Tait equation for the studied FAMEs as a function of pressure along several isotherms

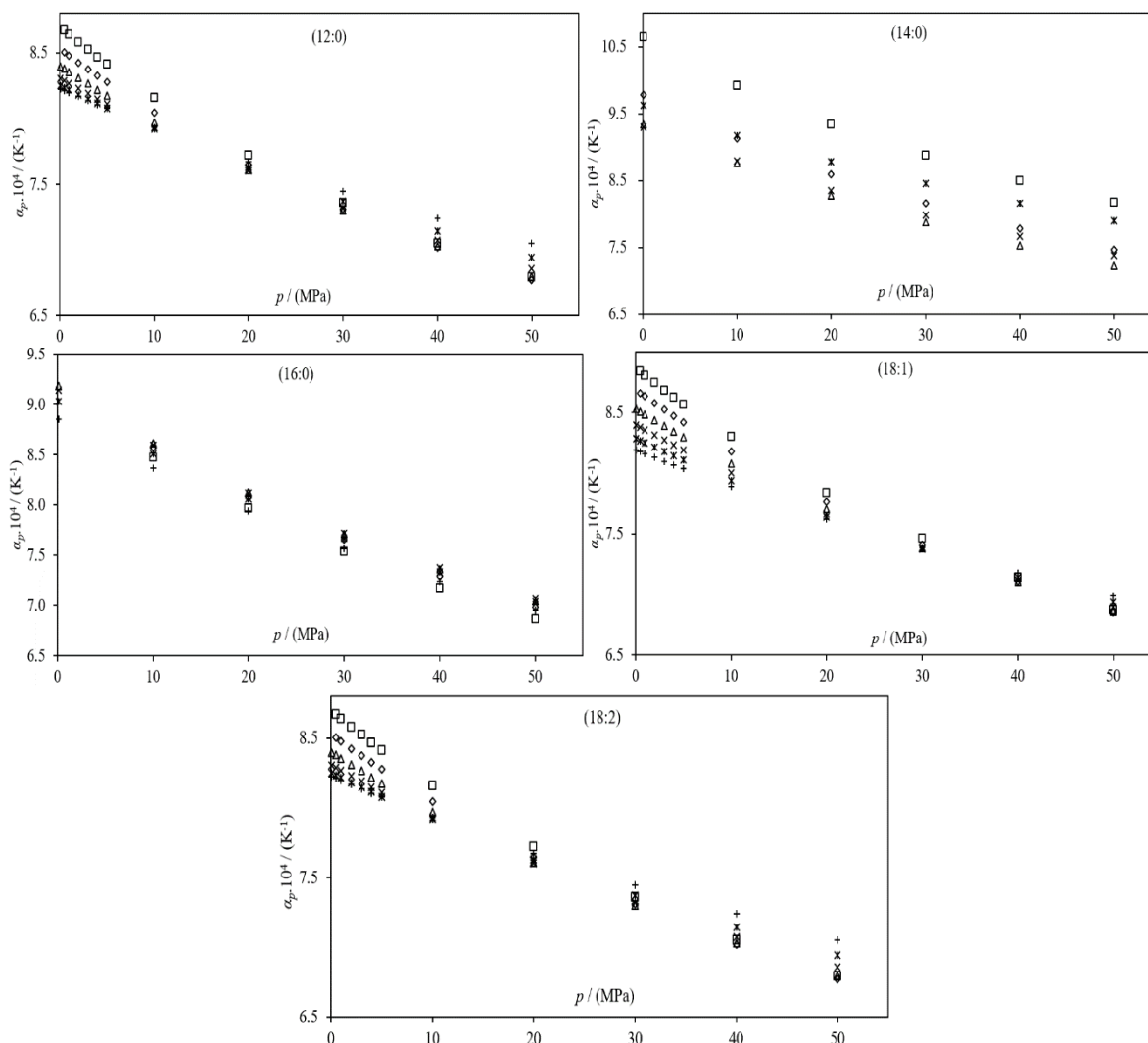


Figure 11: Thermal expansivity, α_p , calculated from Tait equation for the studied FAMEs as a function of pressure along several isotherms. Symbols as in Figure 10

The same behavior is observed for, κ_T , and, α_p , a decrease when the pressure gets higher at constant temperature and an increase when the temperature rises at constant pressure, in consistency with that expected. The isotherms, α_p , had a clear point of intersection. It is important to note that the absence of this point at (18: 2) is probably related to experimental data of density applied in this work, as some authors have shown the presence of this point with precision for many classes of compounds, including FAME [43-46]. This point means that, α_p , was independent of temperature in this pressure because it obeys the condition $(\partial\alpha_p/\partial T)_p = 0$.

Concerning the effect of the alkyl chain length on the derived thermodynamic properties, Figure 12 illustrates a presentation according to the temperature at atmospheric pressure of all the FAME present in this work.



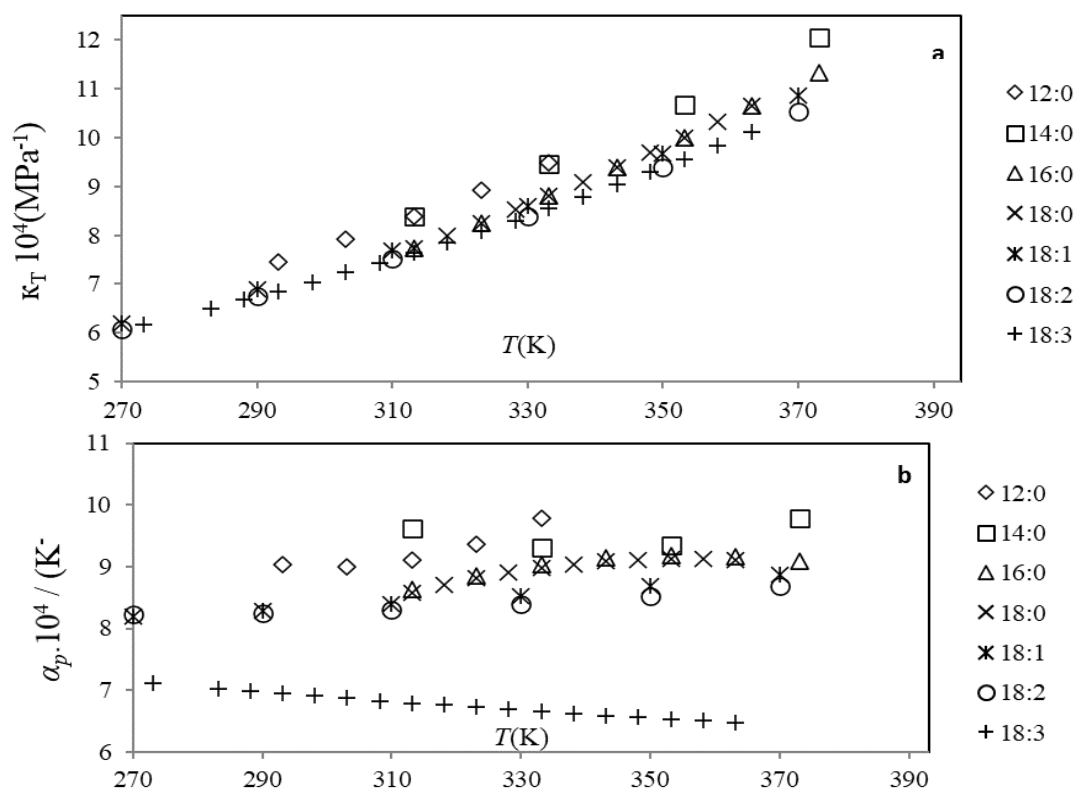


Figure 12: The derived thermodynamic properties for the studied FAMEs calculated from Tait EoS as a function of temperature at atmospheric pressure: (a) Isothermal compressibility, κ_T , (b) Thermal expansivity, α_p .

As seen in the figure, the derived properties, κ_T , or, α_p , of all FAME decrease with the length of the fatty acid chain and with the unsaturation degree. In addition, the α_p curves show a thermal stability domains at atmospheric pressure depending on the nature of studied FAME. for example, FAME (12: 0) shows a thermal stability range between 290 K and 303 K, (18: 2) shows a thermal stability range between 270 K and 310 K, (16: 0) shows a thermal stability range between 343.15 K and 363.15 K. It was interesting to note that this information is of major importance because a larger isobaric expansivity coefficient means a larger engine power loss due to fuel heating [47].

Conclusion

The densities of seven FAMEs were compiled under temperature conditions between 270 K and 393.15 K and at pressures up to 80 MPa. As expected, the density of FAME decreases with temperature and increases when the pressure increases at a constant temperature. The results suggest a relationship between molecular weight, fatty acid methyl ester type (saturated or unsaturated), and temperature, as dependent variables of the density. The PR, Tait and PC-SAFT models are used to predict and correlated the density methyl esters, the parameters of tait and PC-SAFT models were adjusted using the experimental data and for PR EoS, the critical parameters: T_c , p_c and acentric factors, ω , were selected using a comparative study based on several previous works of literature. The Tait and PC-SAFT models represent and correctly reproduce the density of the of fatty acid methyl ester compounds, despite that PC-SAFT requires fewer parameters than Tait equation, but the methodologies that use cubic equations of state (such as Peng–Robinson) must be not safe for the evaluation of complex fluids properties. The derived thermodynamic properties, i.e. isobaric thermal expansion coefficient, α_p , and the isothermal compressibility coefficient, κ_T , were calculated from the experimental density data using the Tait equation. The coefficient of thermal expansion α_p follows a similar behavior of κ_T . However, for α_p a clear point of intersection is observed for each compound, this point means that, α_p was independent of temperature in this pressure because it obeys the

condition $(\partial \alpha_p / \partial T)_p = 0$.



References

- [1]. C. M. P. Pereira; C. B. Hobuss; J. V. Maciel, L. R. Ferreira; F. B. Del Pino; M. F. Mesko; E. Jaboc-Lopes; P. Colepicolo Neto. Biodiesel derived from microalgae: advances and perspectives. *Quim. Nova.* 35 (2012) 2013-2018.
- [2]. R. Megargle, ASTM (American Society for Testing and Materials) standards for medical computing, *Comput. Healthc.* 11 (1990) 25-26.
- [3]. W. Ting; C. Huang; N. Giridir; W. Wu, An enzymatic/acid-catalyzed hybrid process for biodiesel production from soybean oil. *J. Chin. Inst. Eng.* 39 (2008) 203-210.
- [4]. N. H. Dong; N. T. Thuy; V. D. S. Tho, Predicting the temperature/pressure dependent density of biodiesel fuels, *Petro Vietnam. J.* 10 (2012) 46-58.
- [5]. M. J. Pratas; M. B. Oliveira; M. J. Pastoriza-Gallego; A. J. Queimada; M. M. Pineiro and J. A. Coutinho. High-pressure biodiesel density: experimental measurements, correlation, and cubic-plus-association equation of state (CPA EoS) modeling. *Energ. Fuel.* 25 (2011) 3806-3814.
- [6]. E. H. I. Ndiaye; M. Habrioux; J. A. Coutinho; M. L. Paredes and J. L. Daridon. Speed of sound, density, and derivative properties of ethyl myristate, methyl myristate, and methyl palmitate under high pressure. *J. Chem. Eng. Data.* 58 (2013) 1371-1377.
- [7]. M. J. Pratas; S. Freitas; M. B. Oliveira; S. C. Monteiro; A. S. Lima and J. A. Coutinho. Densities and viscosities of fatty acid methyl and ethyl esters *J. Chem. Eng. Data.* 55 (2010) 3983-3990.
- [8]. S. L. Outcalt. Compressed-liquid density measurements of methyl oleate and methyl linoleate. *J. Chem. Eng. Data.* 56 (2011) 4239-4243.
- [9]. M. J. Pratas; S. Freitas; M. B. Oliveira; S. C. Monteiro; Á. S. Lima and J. A. Coutinho. Densities and viscosities of minority fatty acid methyl and ethyl esters present in biodiesel. *J. Chem. Eng. Data.* 56 (2011) 2175-2180.
- [10]. M. L. Huber; E. W. Lemmon; A. Kazakov; L. S. Ott; T. J. Bruno, Model for the Thermodynamic Properties of a Biodiesel Fuel. *Energ. Fuels.* 23 (2009) 3790-3797.
- [11]. P. Hegel; A. Andreatta; S. Pereda; S. Bottini; E. A. Brignole. High pressure phase equilibria of supercritical alcohols with triglycerides, fatty esters and cosolvents. *Fluid Ph. Equilibria.* 266 (2008) 31-37.
- [12]. M. B. Oliveira; A. R. R. Teles; A. J. Queimada; J. A. P. Coutinho. Phase equilibria of glycerol containing systems and their description with the Cubic-Plus-Association (CPA) Equation of State. *Fluid Ph. Equilibria.* 280 (2009) 22-29.
- [13]. Y. Shimoyama; T. Abeta; L. Zhao; Y. Iwai. Measurement and calculation of vapor-liquid equilibria for methanol + glycerol and ethanol + glycerol systems at 493-573K. *Fluid Ph. Equilibria.* 284 (2009) 64-69.
- [14]. O. Ferreira; E. A. Brignole; E. A. Macedo, Modelling of phase equilibria for associating mixtures using an equation of state. *J. Chem. Thermodynamics.* 36 (2004) 1105-1117.
- [15]. M. V. Pena; F. F. M. Azevedo; M. E. Araújo, Cálculo do Equilíbrio de Fases de Constituintes da Transesterificação Enzimática de Óleos Vegetais em Dióxido de Carbono Pressurizado. 1º Congresso Brasileiro de Tecnologia de Biodiesel: Artigos Técnico Científicos. 2 (2006) 235-240.
- [16]. L. Cheng; Y. Cheng; S. Yen; J. Chen. Application of UNIQUAC and SVM to ultrafiltration for modeling ternary mixtures of oil, FAME and methanol. *Chem. Eng. Sci.* 64 (2009) 5093- 5103.
- [17]. P.M. Ndiaye; E. Franceschi; D. Oliveira; C. Dariva; F.W. Tavares; J. V. Oliveira. Phase behavior of soybean oil, castor oil and their fatty acid ethyl esters in carbon dioxide at high pressures. *J. Supercrit. Fluid.* 37 (2006) 29-37.
- [18]. F. E. Alaoui M'hamdi, E. A. Montero; G. Qiu; F. Aguilar and J. Wu. Liquid density of biofuel mixtures: 1-heptanol+ heptane system at pressures up to 140 MPa and temperatures from 298.15 K to 393.15 K. *J. Chem. Thermodyn.* 65 (2013) 174-183.



- [19]. D. Y. Peng; D. B. Robinson. A new two-constant equation of state. *Ind. Eng. Chem. Fund.* 15 (1976) 59-64.
- [20]. K. G. Joback; R. C. Reid; Estimation of Pure-Component Properties from Group-Contributions. *Chem. Eng. Comm.* 57 (1987) 233-243.
- [21]. V. Anikeev; D. Stepanov; A. Yermakova. Thermodynamics of phase and chemical equilibrium in the process of biodiesel fuel synthesis in subcritical and supercritical methanol. *Ind. Eng. Chem. Res.* 51 (2012) 4783-4796.
- [22]. J. Marrero; R. Gani. Group-contribution based estimation of pure component. *Fluid Ph. Equilibria.* 183-184 (2001) 183-208.
- [23]. B. X. Han; D. Y. Peng. A group-contribution correlation for predicting the acentric factors of organic compounds. *Can. J. Chem. Eng.* 71 (1993) 332-334.
- [24]. D. Ambrose; J. Walton. Vapour pressures up to their critical temperatures of normal alkanes and 1-alkanols. *Pure Appl Chem.* 61 (1989) 1395.
- [25]. W. G. Chapman; G. Jachson; K. E. Gubbins. Phase equilibria of associating fluids. Chain molecules with multiple bonding sites. *Mol. Phys.* 65 (1988) 1057.
- [26]. J. Gross; G. Sadowski. Perturbed-Chain SAFT: An Equation of State Based on a Perturbation Theory for Chain Molecules. *Ind. Eng. Chem. Res.* 40 (2001) 1244-1260.
- [27]. G. Tammann, *Z. Phys. Chem.* 17 (1895) 620
- [28]. Wohl, A., *Z. Phys. Chem.* 1 (1921) 234.
- [29]. A. T. J. Hayward, Compressibility equations for liquids: a comparative study. *J. Appl. Phys.* 18 (1967) 965.
- [30]. I. Cibulka, M. Ziková. Liquid Densities at Elevated Pressures of 1-Alkanols from C1 to C10: A Critical Evaluation of Experimental Data, *J. Chem. Eng. Data.* 39 (1994) 876-886.
- [31]. C.A. Cerdeirina, C.A. Tovar, D. Gonzalez-Salgado, E. Carballo, L. Romaní, Isobaric thermal expansivity and thermophysical characterization of liquids and liquid mixtures, *Phys. Chem. Chem. Phys.* 3 (2001) 5230-5236.
- [32]. J. Troncoso, D. Bessieres, C.A. Cerdeirina, E. Carballo, L. Romaní, Automated Measuring Device of (P, ρ , T) Data: Application to the 1-hexanol|N-Hexane System. *Fluid ph. equilibria.* 208 (2003) 141-154.
- [33]. X. Wang; K. Kang; S. Zhu and B. Gao. High-pressure liquid densities of fatty acid methyl esters: Measurement and prediction with PC-SAFT equation of state. *Fluid Ph. Equilibria.* 471 (2018) 8-16.
- [34]. M. L. Corazza; W. A. Fouad and W. G. Chapman. PC-SAFT predictions of VLE and LLE of systems related to biodiesel production. *Fluid Ph. Equilibria.* 416 (2016) 130-137.
- [35]. N. Von Solms; M. L. Michelsen; G. M. Kontogeorgis. Prediction and correlation of high-pressure gas solubility in polymers with simplified PC-SAFT. *Ind. Eng. Chem. Res.* 44 (2005) 3330-3335.
- [36]. F. T. Peters; F. S. Laube; G. Sadowski, Development of a group contribution method for polymers within the PC-SAFT model. *Fluid Ph. Equilibria.* 324 (2012) 70-79.
- [37]. K. Chakravarthy; J. McFarlane; S. Daw; Y. Ra; R. Reitza and J. Griffin. Physical properties of bio-diesel and implications for use of bio-diesel in diesel engines. *SAE Transactions.* (2007) 885-895.
- [38]. H. An; W. M. Yang; A. Maghbouli; S. K. Chou and K. J. Chua. Detailed physical properties prediction of pure methyl esters for biodiesel combustion modeling. *Appl. Energy.* 102 (2013) 647-656.
- [39]. S. Baroutian; M. K. Aroua; A. A. Raman and N. M. N. Sulaiman. Density of palm oil-based methyl ester. *J. Chem. Eng. Data.* 53 (2008) 877-880.
- [40]. T. Wallek; J. Rarey; J. O. Metzger and J. Gmehling. Estimation of pure-component properties of biodiesel-related components: fatty acid methyl esters, fatty acids, and triglycerides. *Ind eng chem res.* 52 (2013) 16966-16978.
- [41]. P. Saxena; J. C. Patel and M. H. Joshipura. Prediction of vapor pressure of fatty acid methyl esters. *Procedia Eng.* 51 (2013) 403-408.



- [42]. F. R. do Carmo; N. S. Evangelista; F. A. Fernandes and H. B. de Sant'Ana. Evaluation of Optimal Methods for Critical Properties and Acentric Factor of Biodiesel Compounds with Their Application on Soave-Redlich-Kwong and Peng–Robinson Equations of State. *J. Chem. Eng. Data.* 60 (2015) 3358-3381.
- [43]. P.W Bridgman. *The physics of high pressure: Dover Publications, New York, 1970.*
- [44]. N. M. Prieto; A. G. Ferreira; A. T. Portugal; R. J. Moreira; J. B. Santos. Correlation and prediction of biodiesel density for extended ranges of temperature and pressure. *Fuel.* 141 (2015) 23-38.
- [45]. A. Schedemann; T. Wallek; M. Zeymer; M. Maly; J. Gmehling. Measurement and correlation of biodiesel densities at pressures up to 130 MPa. *Fuel.* 107 (2013) 483-492.
- [46]. M. Taravillo; V. G. Baonza; M. Cáceres; J. Núñez. Thermodynamic regularities in compressed liquids: I. The thermal expansion coefficient. *Phys. Condens. Matter.* 15 (2003) 2979.
- [47]. R. Aitbelale; I. Abala; F. E. M'hamdi Alaoui; A. Sahibeddine; N. Munoz Rujas and F. Aguilar. Characterization and determination of thermodynamic properties of waste cooking oil biodiesel: Experimental, correlation and modeling density over a wide temperature range up to 393.15 and pressure up to 140 MPa. *Fluid Ph. Equilibria.* 497 (2019) 87-9

